doi:10.14311/ppt.2025.1.22
Plasma Physics and Technology **12**(1):22–27, 2025

EXPERIMENTAL VALIDATION OF MHD ARC SIMULATION IN ENCAPSULATED HORN GAP ARRANGEMENTS

A. Ehrhardt[a], S. Schmausser[a,*], O.Schneider[a], D. Gonzalez[b]

[a] *DEHN SE, Hans-Dehn-Straße 1, 92318 Neumarkt, Germany*

[b] *Leibniz Institute for Plasma Science and Technology, Felix-Hausdorff-Straße 2, 17489 Greifswald, Germany*

[*] sebastian.schmausser@dehn.de

Abstract. This work describes the use of experimental methods on model spark gaps for comparison with the simulation models (MHD) from the ignition of the impulse arc to the entry of the arc into the arc chamber, taking into account material effects and thermal reignitions of the arc, e.g. as a result of the gas flow within the encapsulated spark gap. Examples are provided to show that the simulation can accurately represent the experimental processes and improve the understanding of the complex processes.

Keywords: arc simulation, spark gap, impulse current, follow current.

1. Introduction

The physical processes that lead to a rapid and safe interruption of the arc in an encapsulated horn spark gap for low-voltage grids are complex. The influencing factors are manifold and experimental investigations require a great deal of effort. The investigation of the dynamic pressure and flow conditions within the spark gap can only be carried out with difficulty or insufficiently, e.g. by optical methods, without influencing the arc behavior. For further optimization of such spark gaps, a complex simulation is useful. The simulation shall depict with sufficient accuracy the ignition of the spark gap by an impulse arc, the transition to the network-driven arc, the movement and arc splitting in the extinguishing chamber, as well as the arc interactions with the materials and geometry of the spark gap. For this purpose, the model assumptions of the simulation are to be successively compared with suitable experiments on reproducible and variable model spark gaps in order to enable further optimization of the spark gap with significantly reduced experimental effort.

Lightning arresters respond to overvoltages in the low-voltage grid [1]. In the case of high-energy surge loads, an arc discharge is ignited in the separation gap by the ignition device of the spark gap. After the surge has been dissipated, currents can also flow from the grid, so-called grid follow currents, via this low-impedance path. To prevent that the superordinate overcurrent protection devices of the low-voltage grid need to respond as a result of this low-impedance connection, the lightning arrester shall permit to quickly limit the mains follow current and extinguish the arc.

To guarantee a reliable function, the considered spark gaps have an ignition device, an built-in arc running area and a deion extinguishing chamber [2]. Modern lightning current arresters have overvoltage protection levels of < 1.5 kV, can safely extinguish short-circuit currents in DC and AC networks, prevent the release of hazardous gases, and are designed to be very space-saving [2]. The limitation of follow currents is achieved by extending and splitting the arc, similar to a low-voltage circuit breaker. However, spark gaps have fixed electrodes with only a small distance in the ignition area. Therefore, there is no minimum extension of the arc through the movement of a switching contact.

Another difference from switches is the higher amount of energy delivered by the surge at the ignition region with impulse current arcs with magnitudes of several tens of kA, which cannot be limited like follow currents by the function of the spark gap and show therefore an impressed nature. The propagation and energy release of these impulse arcs leads to changes in the starting conditions for the limitation of follow currents.

This influence should be sufficiently accurately considered for the further optimization of the lightning current arresters in a simulation model.

In [3], a simulation model for the behavior of a follow current arc in a spark gap with diverging electrodes and an extinguishing chamber was described. The simulation was carried out using the CFD code FlowVision [4] and the integrated MHD approach based on the Finite Volume Method (FVM).

The simulation in [3] showed that the behavior of a follow current arc can be represented with sufficient accuracy. However, only a simple radiation model (P1 gray) was used in the simulation in [3]. Ablation processes were not considered in that work. The ignition of the spark gap in the experiments is achieved through a very low-energy impulse current of low amplitude, which allowed the energy input and its influence on the subsequent follow current to be neglected in the experiment. In the simulation, the arc ignition was carried out with the assumption of a high-temperature cylinder, whose geometry and position were aligned

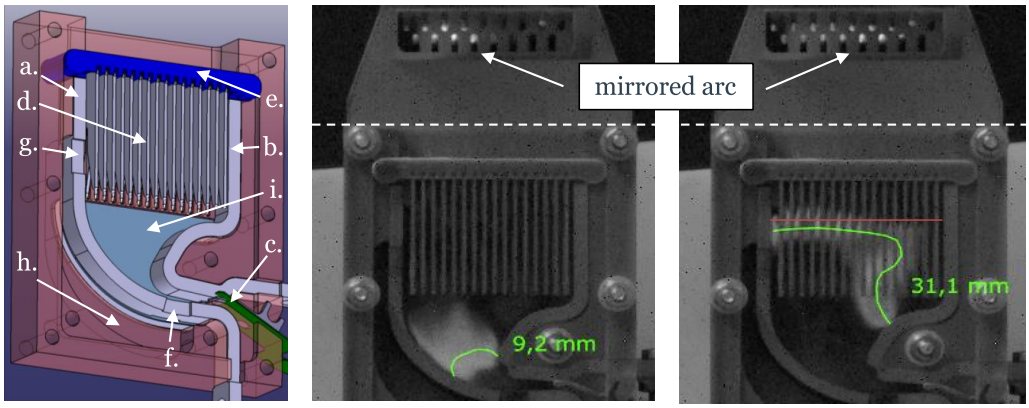

Figure 1. CAD model of the spark gap (left) and highspeed camera recordings for the investigation of arc geometry and voltage requirements with lateral and frontal (mirror) observation (middle and right).

with that observed by the experiments. The simulation of the impulse arc was not performed in [3] due to the lack of required model assumptions.

In [5], the simulation of an impulse arc for the lightning current arrester is presented and compared with experimental investigations. The simulation in FlowVision was extended with the discrete ordinates method (DOM) in a spectral approximation with pressure dependence. Additionally, corresponding temperature- and pressure-dependent plasma properties [5] as well as data on radiation bands from the literature were used, comparative calculations were carried out, and the most suitable [6] data regarding the result and computation time were supplemented in FlowVision.

The calculation of the impulse arc with the simplifying assumption of Local Thermal Equilibrium (LTE) for the plasma state still provides sufficient accuracy in the considered current range up to 5 kA. The movement, speed, expansion, pressure, and temperature of the simulated impulse arc show good agreement with the experimental results under the assumptions made.[5]

In this work, experiments will be conducted to investigate the transition from impulse current to follow current arc, as well as reignitions of spark gaps before the stable entry of the arc into the quenching chamber. An accompanying simulation based on previous modeling approaches [5, 6] will show to which extent these processes can already be represented, and what improvements are still necessary.

2. Model spark gaps for experimental investigations

To align the simulation with the experiments, several requirements arise for the model spark gaps:

- ☐ simple construction (reduction of FV elements),
- ☐ optical observation of the arc,
- ☐ multiple electrical loads of small and medium impulse and follow currents reproducible possible (robustness).

The goals of the experiments include determining

- ☐ transition from impulse current arc to follow current arc (location, geometry),
- ☐ arc running on the electrodes (geometry, speed),
- ☐ influence of wall gas emission,
- ☐ reignition behavior (geometry, location, voltage differences).

For the models, spark gaps with diverging electrodes made of stainless steel or copper (a. and b. in Figure 1) with an ignition aid (c.), which is arranged between the electrodes, were chosen. The electrodes function as running rails. Each spark gap has an extinguishing chamber with 16 extinguishing plates (d.). The extinguishing chamber has a damping of about 50% (e.). For the consideration of the reignition behavior, a damping of 100% can be used.

One of the electrodes also has two pairs of openings (f. and g.), which allow gas circulation through a cavity (h.) next to the electrode. The notches are in the area of the ignition device and in the entry area of the deionization chamber (Fig. 1). The effect of gas circulation under follow current load was already pointed out in [3]. The spark gaps have mounts next to the electrodes, allowing to change the material of the lateral boundary (i.) of the arc running area. This enables the spark gaps to be optionally equipped with transparent side walls, allowing lateral observation of the arc in the relevant functional area. Additionally, the choice of material can vary the gas emission of the lateral arc boundary.

In addition to the transparent side walls, a mirror with a 45° angle can be mounted above the damping (Fig. 1), allowing for both lateral and frontal observation of the arc. This enables a better assessment of the arc geometry even in the depth of the arc chamber.

To assess the voltage requirements during arc splitting, the geometry (entry area, length) of the extinguishing plates and the material can also be varied. For the analysis of arc behavior, an highspeed camera with various lenses and filters is used. The arc

brightness (no overexposure) and the filter characteristics are used for a rough estimation of the arc dimensions. As a direct comparison of recordings with simulation results is difficult [7], line filters are used in this work to limit the observation to the emission of given species that can only be present within the arc or in its immediate boundary area.

3. Transition from impulse arc to follow current arc

In [5], the good agreement between the experimental investigations with an impulse arc of 5 kA with a waveform of 8/20 µs and the simulation was shown. If the spark gap is simultaneously connected to an electrical network, this network can drive a follow current through the spark gap after ignition due to overvoltage. A corresponding test circuit is shown in Figure 2. The impulse current source has a very high driving voltage compared to the rated grid voltage, which causes the impulse current to dominate the arc behavior at the beginning. For the used surge source, the waveform 8/20 µs does not result in an aperiodic course, but the impulse current can change polarity multiple times. This can cause the arc in the spark gap to extinguish and reignite multiple times.

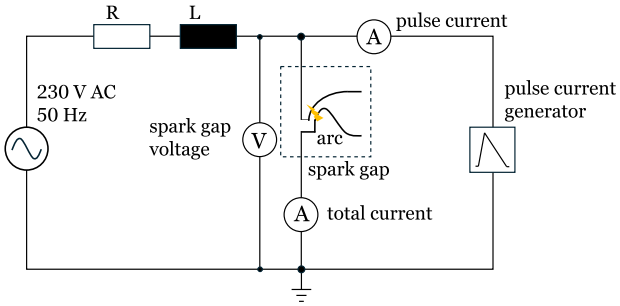

Figure 2. Test circuit for follow current investigations (prospective current $I_p = 1.3\ kA$, $cos\phi = 0.8$).

After the impulse current decays, the arc is fed exclusively by the grid. The impulse current spreads according to its current strength within the running area of the spark gap and partially moves along the electrodes. This results in an increase in temperature and ablation of the spark gap components (electrodes, wall material). Additionally, pressure waves are caused due to the abrupt gas displacement. These effects further influence the behavior of the follow current arc, from the formation of the conductive channel, through the movement along the electrodes to its extinction. The spark gap in the test circuit is rotated 90° clockwise compared to Figure 1. This orientation is maintained in the subsequent figures.

For the simulation of the actual process, it is therefore relevant that the transition from impulse arc to follow current arc can be represented with sufficient accuracy and as seamlessly as possible. The temporal evaluation of the arc spectrum (Fig. 3) with spark gaps as in [8] showed no significant differences between the spectra in measurements with only impulse current or measurements with impulse and follow current, which would indicate the occurrence of new species or the increase in proportions of, for example, Cu or C. These results are valid during the decay of the 5 kA impulse current (between 12 and 25 µs) and correspondingly also for the superimposed follow currents in the range of 2–5 kA, building on the results presented in [8]. Furthermore, the results in [8] indicate a LTE for the plasma of the surge arc, in particular during current decay. Consequently, the follow current arc was calculated in the first simplification using the models presented in [5] for describing the impulse arc.

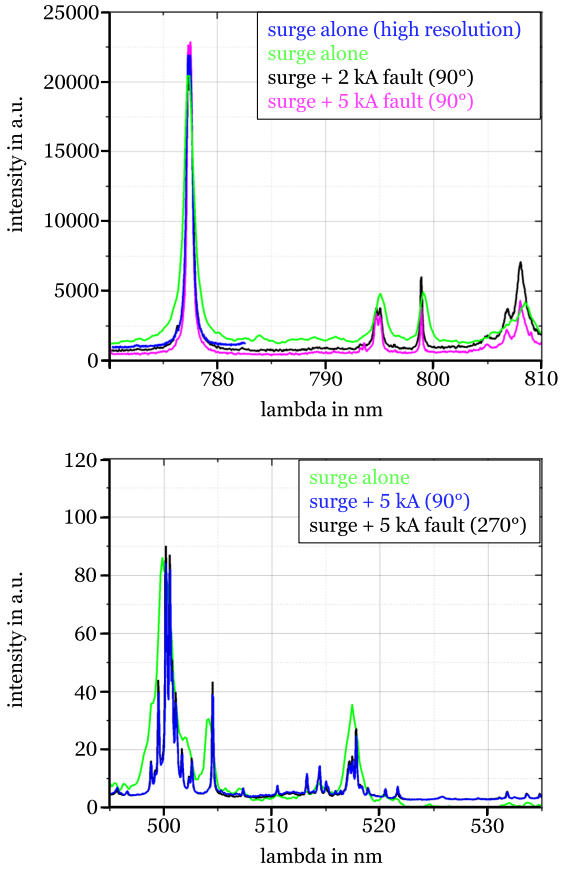

Figure 3. Comparison of lines in the evaluated range between 770 nm – 810 nm and 495 nm – 535 nm.

In Figure 4, highspeed recordings and a simulation of the arc in the relevant time range are shown. The simulated arc is represented here as current density and overlaid with vectors depicting the gas flow. Figure 4 a. is at the back of the trigger impulse and shows the retracting impulse current arc, which subsequently extinguishes at the zero crossing. At this point, a follow current from the power grid is already flowing, which is small compared to the impressed impulse current, and the arc is therefore dominated by former. Due to the undershoot, another impulse arc with reversed current direction is formed (Fig. 4 b.). After another zero crossing, another impulse arc ignites with the original current direction. Figure 4

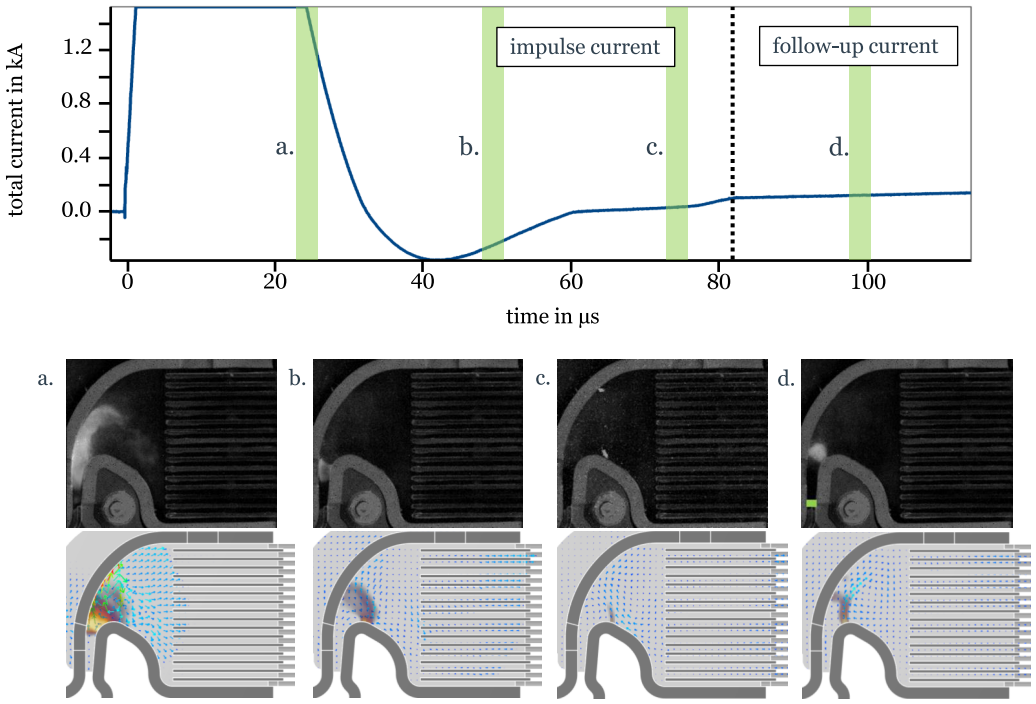

Figure 4. Highspeed camera recordings and simulation of the transition from impulse current to follow current. In d., the ignition point of the impulse current arc is marked in green. The simulated arc in current density representation (range from 1×10^7 to $1 \times 10^8 A/m^2$) is overlaid with vectors depicting the direction and speed of the gas flow.

c. shows the beginnings (foot points) of the already extinguishing arc at the electrodes. In Figure 4 d., a pure follow current arc can be seen, which is fed exclusively by the current from the grid. Even with this still low and energy-poor impulse current, it can be seen that the reignitions and thus the transition to the follow current are strongly influenced by the behavior and energy input of the preceding impulse current. Due to the expansion and movement of the impulse arc beyond its ignition point, the spark gap in this region is already heated and gas flow is stimulated. This thus influences the further behavior during the impulse current discharge and also the follow current arc.

The position of the arc in Figure 4 d. differs both in the experiments and the simulation from the ignition position of the arc during the impulse discharge. Therefore, it is advantageous to directly simulate the reignitions of the impulse arc and the transition to the follow current arc using the software. On the one hand, interrupting the simulation and specifying the ignition position of the follow current arc analogously to the ignition of the impulse arc would be associated with a larger error, especially at higher impulse currents. On the other hand, an independent simulation of the transition allows for a complete physical consideration of the actual phenomena occurring in the plasma and the interaction with the feeding current source regarding the resulting current-limiting effects. However, the simulation is still limited by the accuracy and completeness of the material data and the radiation model.

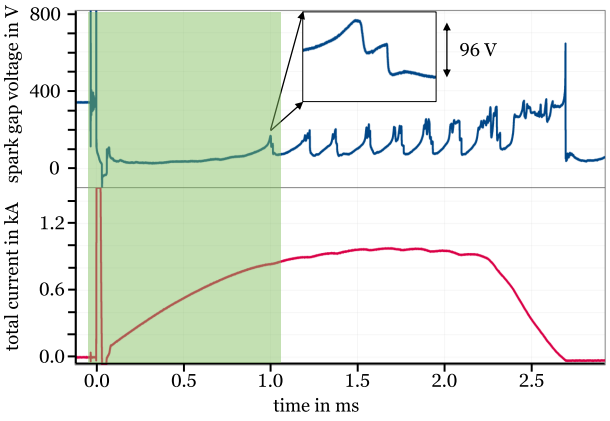

Figure 5. Measured current-voltage curve on a spark gap with strong gas emission and complete damping. The green area was replicated in the simulation.

4. Investigations into reignitions of the follow current arc

Of equal importance to the correct representation of the transition from impulse current arc to follow current arc is the ability to simulate reignition processes. Reignitions of the arc to low voltage values can increase the conduction current and interruption integrals in spark gaps. The increase in these values stresses the overcurrent protection elements of the grid and can therefore lead to their tripping and thus to the interruption of the power supply. Therefore, the reduction of reignitions should be considered in further development. It is essential that the simulation program can accurately represent the reignition oc-

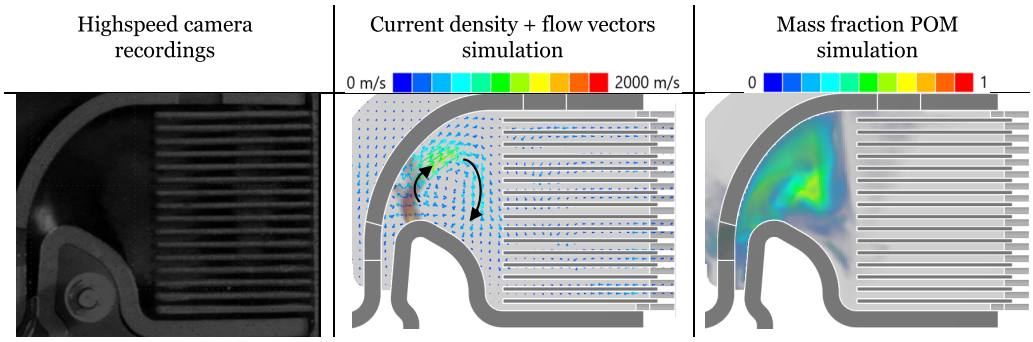

Figure 6. Recording at the beginning of the pure follow current arc as well as flow velocity and POM gas content from the simulation.

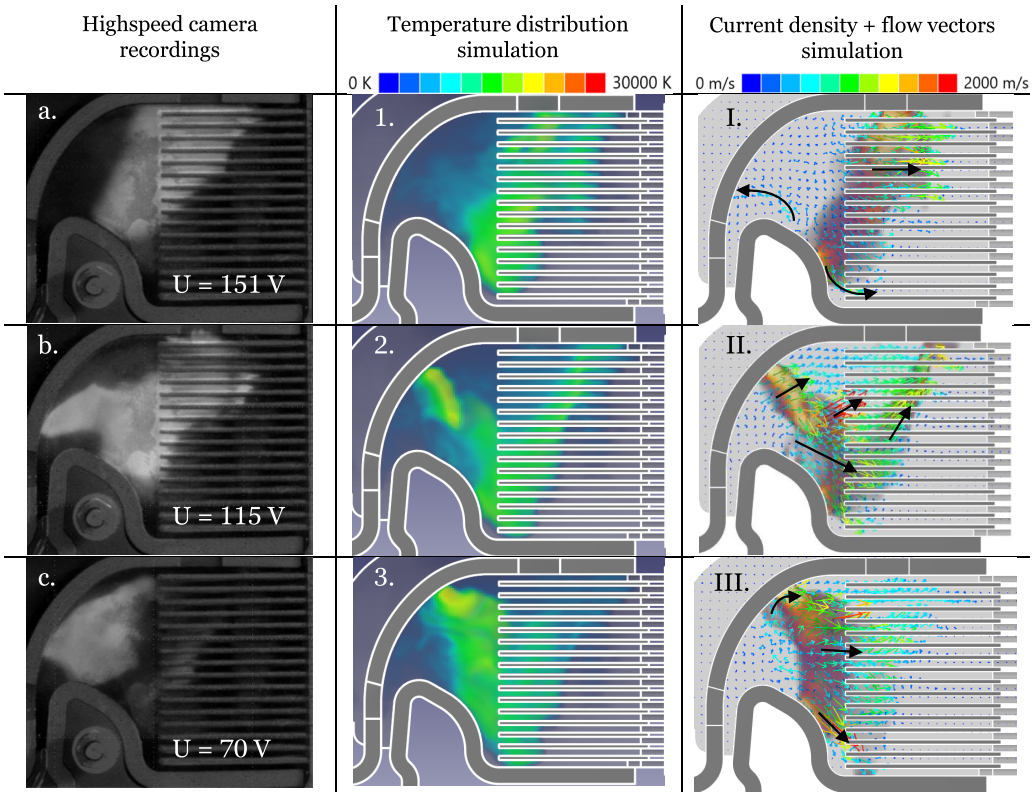

Figure 7. Comparison of the recorded and simulated arc before, during, and after reignition.

curence. In real spark gaps, reignitions are associated with a certain degree of randomness due to several influencing factors. The effort to experimentally capture and observe these with sufficient accuracy is therefore quite high. To make investigations feasible with reasonable effort, the spark gaps were modified so that reignitions occur with high probability. By using strongly outgassing wall material, the pressure build-up below the arc chamber is significantly increased and the turbulence of the flow, especially of the hot gases, is intensified. Additionally, the damping of the arc chamber was increased to 100%, allowing multiple reignitions to be generated in the experiment over a longer period. The additional gas emission from the walls was considered in the simulation by incorporating an ablation model. For simplification, POM [9] was assumed as the wall material in the simulation. Due to the very intense energy release of the higher impulse current, the stronger gas emission of POM compared to vulcanized fiber will, in this case, lead to a certain exaggeration of the gas emission effect, which, however, better illustrates the influence of the relevant flows in the spark gap. For loads investigated, ablation does not cause changes in geometry.

By triggering the model spark gap with an impulse current of 5 kA 8/20 µs and enhancing the gas emission, reignitions can already be observed in the running area of the model spark gap. Figure 5 shows a corresponding measured current-voltage curve.

Due to the complete damping of the spark gap, gas flows develop immediately after ignition (Fig. 6), which counteract the rapid movement of the arc to the arc extinguishing chamber, thereby reducing the arc running speed and even temporarily reversing the

arc's direction of movement. Due to the associated low running speed and arc movement, the arc between the running rails hardly extends. Thus, there is only a slight increase in arc voltage due to extension, which means the current increase as a result of the driving mains voltage can hardly be influenced. Therefore, the intense arc very quickly causes a strong gas release, which additionally intensifies the flow effects in the spark gap. The arc runs delayed and only discontinuously towards the arc chamber, extending during the process. An arc voltage of approximately 100–200 V is already built up as counter-voltage, which is still significantly below the driving voltage of the source ($\hat{U} = 325\,V$). A current limitation does not occur at the voltage reached so far.

Figure 7 shows comparative images of the recorded arc and the simulated arc at various times from ignition to the first reignition, respectively the marked area in Figure 5. The arc recordings show the arc before reaching the first voltage peak (a.), during the reignition process with still two current-carrying arc channels (b.), and at the time of the voltage minimum after the first reignition (c.). Even in this phase, the movement of gases in the spark gap influences the direction and speed of the arc. Due to the low running speed, the backward movements of the arc, and the partially backward movement of the hot gases (Fig. 7 I.), there is only insufficient cooling of the gas volume and the electrodes in the area already traversed by the arc. Below the arc, both the electrodes and the gas space remain strongly heated (Fig. 7 1.), which results in residual conductivity. As the increasing arc voltage during the attempt to enter the arc chamber forcibly leads to an increase in current flow in the still heated areas of the spark gap (Fig. 7 II., left channel), a thermal reignition of the arc finally occurs below its reached position with lower arc voltage (Fig. 7 c., 3. and III.). The original channel (Fig. 7 a., 1. and I.) completely extinguishes in the further course.

The qualitative comparison between the experimental investigations and the simulation shows a sufficient agreement despite the stochastic nature of these processes. Both the time course of current and voltage as well as the spatial reference of the simplified visualization of the arc during reignitions show that these effects can be well described by the simulation model. The visualization capabilities of the simulation also enhance the understanding of the complex interaction of various processes during an arc extinguishing event.

5. Summery and prospects

The investigation shows that the impulse arc, due to its energy input, propagation, and movement in the spark gap, strongly influences the conditions to extinguish follow fault currents. The impulse current, which ignites the spark gap, among other things, affects the location, movement, and conditions for reignitions of the follow current arc. With the solution approaches integrated so far in the CFD software FlowVision, these relevant processes can already be well represented even in the immediate transition from the impulse current arc to the follow current arc.

Furthermore, a detailed comparison of the geometric and electrical data of the arc with the simulation is to be carried out. The pressure- and temperature-dependent material data used are to be further compared with the conditions in the spark gap regarding the induced gas release, the heating of the components, and the partial pre-ionization in the reached spark gap regions (ignition, running, extinguishing chamber). In addition, a review of the approaches used so far for arc movement and arc splitting is planned.

References

[1] A. Ehrhardt and P. Zahlmann. Measurements of pressure and functional characteristics of a surge arrester at lightning impulses and mains follow currents. In *XVIth Symposium on Physics of Switching Arc*, Brno, Czech Republic, 2005.

[2] A. Ehrhardt, S. Schreiter, U. Strangfeld, and M. Rock. Encapsulated lightning current arrester with spark gap and deion chamber. In *XIXth Symposium on Physics of Switching Arc*, Brno, Czech Republic, 2011.

[3] O. Schneider, A. Ehrhardt, B. Leibig, et al. Surge protection device digital prototyping. In *Proceedings of the 30th International Conference on Electrical Contacts*, pages 486–493, Switzerland, 2020.

[4] A. Aksenov, A. Dyadkin, and V. Pkhilko. Overcoming of barrier between cad and cfd by modified finite volume method. In *Proc. 1998 ASME Pressure Vessels and Piping Division Conference*, pages 79–86, San Diego, USA, 1998.

[5] O. Schneider, D. Gonzalez, and A. Ehrhardt. Multiphysical simulation of impulse current arcs in spark gaps for industrial applications. *Plasma Physics and Technology*, 10(3):119–122, 2023. doi:10.14311/ppt.2023.3.119.

[6] R. Fuchs. Numerical arc simulations of radiatively-induced pmma nozzle wall ablation. In *30th International Conference on Electrical Contacts*, Switzerland, 2021.

[7] M. Anheuser, T. Beckert, and S. Kosse. Electric arcs in switchgear - theory, numerical simulation and experiments. In *XIXth Symposium on Physics of Switching Arc*, Brno, Czech Republic, 2011.

[8] M. Baeva, R. Methling, D. Gonzalez, et al. Complementary experimental and simulation-based characterization of transient arcs. *Plasma Physics and Technology*, 10:56–59, 2023. doi:10.14311/ppt.2023.2.56.

[9] Y. Nakano, Y. Tanaka, and T. Ishijima. Consistent calculation from particle composition to arc simulation for arc ignition process in polymer ablated arcs. *Plasma Chemistry and Plasma Processing*, 44(1):1–24, 2023. doi:10.1007/s11090-023-10360-9.